NMR (^{55}Mn, ^{139}La) and Mössbauer Spectroscopy (^{119}Sn) Studies of (La$_{0.67}$Ca$_{0.33}$)(Mn$_{1-x}$Sn$_x$)O$_{3-\delta}$ Compounds

J. Przewoźnik

Department of Solid State Physics
Faculty of Physics and Applied Computer Science
AGH University of Science and Technology
al. Mickiewicza 30, 30-059 Cracow, Poland

Dedicated to Professor Józef Spałek on the occasion of his 60th birthday

A ^{119}Sn Mössbauer spectroscopy and zero field ^{55}Mn and ^{139}La NMR studies of (La$_{0.67}$Ca$_{0.33}$)(Mn$_{1-x}$Sn$_x$)O$_{3-\delta}$ ($x = 0$, 0.01, 0.03, and $\delta \approx 0.06$) were reported. The temperature evolution of the Sn hyperfine field (B_{hf}) for $x = 0.03$ determined from the Mössbauer spectroscopy measurements was analysed within a molecular field model. A fit to the temperature dependence of $B_{\mathrm{hf}}^{\max}$ provided the Curie temperature $T_{\mathrm{C}}^* = 160(3)$ K, which is in good agreement with T_{C} obtained from dc magnetisation measurements. The ^{55}Mn NMR spectra for $x = 0$ and 0.01 show a single double exchange Mn$^{3+/4+}$ resonance line and exhibit strong Suhl–Nakamura relaxation effects characteristic of the ferromagnetic metallic phase. The spectra for $x = 0.03$ show a coexistence of the double exchange line with the lines characteristic of Mn^{3+} and Mn^{4+} valence states. This shows that a 3% Sn doping strongly suppresses the double exchange interaction and leads to microscopic phase segregation into ferromagnetic metal and ferromagnetic insulator.

PACS numbers: 76.60.–k, 76.80.+y, 75.47.Lx, 77.80.Bh, 75.47.Gk

1. Introduction

The optimally doped colossal magnetoresistive (CMR) perovskite La$_{0.67}$Ca$_{0.33}$MnO$_3$ exhibits a first-order metal–insulator (M–I) and concomitant ferromagnetic (FM)–paramagnetic (PM) transitions at the same temperature $T_{\mathrm{M-I}}$ (T_{C}) [1]. The maximal CMR response is observed around this temperature. The basis for the understanding of the simultaneous existence of FM and metallic conductivity in this compound is the concept of the double exchange (DE)

interaction, which is associated with the hopping of the e_g electron between Mn^{3+} ions [2]. Our earlier study of $(La_{0.67}Ca_{0.33})(Mn_{1-x}Sn_x)O_{3-\delta}$ with $x = 0$, 0.01, 0.03, showed that high sintering temperature (1450°C) was necessary to dissolve up to 3 at.% of Sn and it resulted in a large oxygen deficiency δ equal to 0.06 [3]. The vacancies related to positive δ values introduce local structural distortions and cause an increase in Mn^{3+}/Mn^{4+} ratio by amount of 2δ (decrease in the effective hole doping), which shifts our compounds very close to the border line of the stability of the FM metallic state [4]. It is generally accepted that Sn substitutes for Mn^{4+} [5], forming Mn^{3+}/Sn^{4+} pairs which do not support DE interaction. It also introduces local lattice distortions and affects the magnetic, thermal and transport properties of the parent $(La_{0.67}Ca_{0.33})MnO_{3-\delta}$ compound. The vicinity of the border line makes the effect of Sn^{4+} substitution for Mn^{4+} strongly enhanced leading to a strong suppression of T_C and T_{M-I} and a huge departure (66 K for $x = 0.01$) of T_C from T_{M-I} [3, 6].

The aim of the present work was to get a deeper insight into the magnetic and electronic properties of these compounds at the microscopic level via hyperfine interactions by applying local probe methods such as NMR and Mössbauer spectroscopy (MS).

2. Sample preparation

Polycrystalline samples of $(La_{0.67}Ca_{0.33})(Mn_{1-x}Sn_x)O_{3-\delta}$ ($x = 0$, 0.01, and 0.03) were prepared applying the sol-gel method followed by sintering in air at 1450°C for 50 h to ensure that the properties of the compounds vary only due to the different substitution level Sn for Mn. The structural characterization by powder X-ray diffraction (XRD) and by scanning electron microscopy confirmed that Sn was completely dissolved in the structure and good quality compounds with large grains (average diameter 11 μm) were formed [3]. The mass fraction calculated from XRD data by the Rietveld method of the only detected CaO type impurity phase was below 1% in all the compounds. The physical properties of these compounds were discussed extensively elsewhere [3].

3. Results and discussion

3.1. Mössbauer spectroscopy

The ^{119}Sn MS measurements on $(La_{0.67}Ca_{0.33})(Mn_{0.97}Sn_{0.03})O_{2.94}$ compound were performed in the transmission geometry using a constant acceleration type spectrometer and employing $Ba^{119}SnO_3$ as the source. From 15 K to room temperature (RT) the absorber was kept in a cryodyne refrigeration system (CTI--Cryogenics) and the source at RT. The estimated value of the effective absorber thickness T_a for single line paramagnetic spectra was about 1.2. To determine the distribution of the magnetic hyperfine fields in the magnetically split spectra, a program based on the method developed by Hesse and Rübartch [7] and Le Caer and Dubois [8] was used.
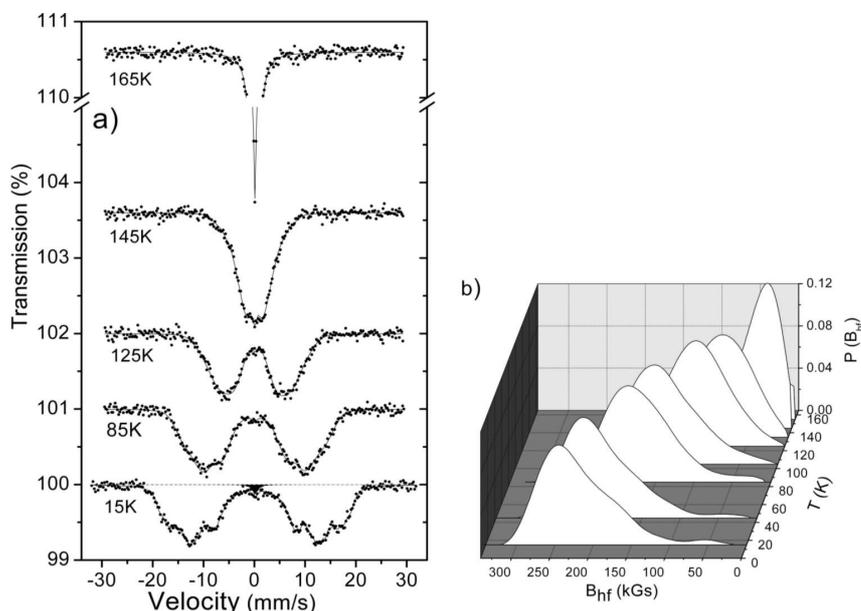
Fig. 1. (a) Temperature variation of the selected $(La_{0.67}Ca_{0.33})(Mn_{0.97}Sn_{0.03})O_{2.94}$ Mössbauer spectra. Solid lines denote the best fits and small black area (at 15 K spectrum) denotes the fitted contribution of the paramagnetic impurity phase. The base lines of the $T > 15$ K spectra are arbitrarily off-set. (b) Temperature dependence of $P(B_{hf})$ obtained from the Mössbauer spectra.

The temperature evolution of the Mössbauer spectra is shown in Fig. 1a. The six-line spectrum measured in the FM state at 15 K shows a strong broadening of all lines. This indicates that a static distribution of the values of the magnetic hyperfine fields (B_{hf}) exists at this temperature. With increasing temperature a gradual decrease in the magnetic splitting of the spectra is observed. Finally, the spectrum collapses into the "single" line (in fact this is a non-resolved quadrupole doublet) paramagnetic spectrum for temperatures higher than 160 K. One can note the existence of a small paramagnetic line in the centre of the spectrum measured at 15 K (the same peak was seen in the spectra measured at higher temperatures). The contribution of this paramagnetic impurity phase, denoted by small black area, amounts to 1.6(3)%. A similar but stronger additional line was observed in the Mössbauer spectra measured for compounds containing an unidentified tin-rich impurity phase [6]. Another possibility is that this small paramagnetic line originates from the CaO type impurity phase detected in this compound in amount of 0.4(2)% [3]. It was natural to subtract this impurity line (assuming the same parameters and relative contribution as in 15 K spectrum) from all the measured spectra to obtain undistorted spectra for the $(La_{0.67}Ca_{0.33})(Mn_{0.97}Sn_{0.03})O_{2.94}$ phase. These "refined" spectra, shown in Fig. 1a for temperatures higher than

15 K, were further analysed. The paramagnetic spectrum measured at 165 K was fitted well with a single quadrupole doublet as shown in Fig. 1a. The doublet has the following hyperfine parameters: isomer shift IS = 0.112(3) mm/s, quadrupole splitting QS = 0.179(8) mm/s (IS values are given as relative to $Ba^{119}SnO_3$ at RT) and line half-width Γ = 0.466(7) mm/s. The IS parameter shows a typical small value of Sn^{4+}, while the nonzero QS value originates from the orthorhombic distortion of the ideal perovskite structure. A contribution of the PM phase was taken into account in the analysis of the FM spectra measured at temperatures lower than 165 K assuming the same values of QS and Γ parameters as in the PM spectrum measured at 165 K. One should mention that nearly zero values of the first-order perturbation theory quadrupole shift parameter ϵ were found for these FM spectra. The hyperfine field probability density functions $P(B_{hf})$ determined from the spectra measured up to 155 K are shown in Fig. 1b. In the whole temperature range a wide and asymmetric distribution of B_{hf} takes place. The presented probability density functions, $P(B_{hf})$, allowed us to calculate such parameters as mean value, $\langle B_{hf} \rangle$, standard deviation of the mean value, σ $(= \sqrt{\langle (B_{hf} - \langle B_{hf} \rangle)^2 \rangle})$, as well as to determine the maximum value B_{hf}^{max} (defined as the extrapolation of the maximal slope of the $P(B_{hf})$ curve to the B_{hf} axis). These parameters, together with the fitted relative contribution of the PM fraction to the spectra are plotted versus temperature in Fig. 2a. The $\langle B_{hf} \rangle$ and B_{hf}^{max}
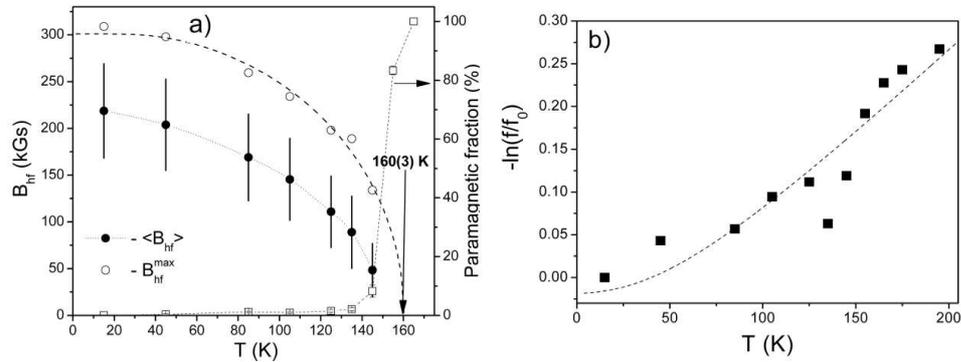
Fig. 2. (a) Temperature dependence of $\langle B_{hf} \rangle$ (full circles), B_{hf}^{max} (open circles), σ (vertical lines around $\langle B_{hf} \rangle$ values) and paramagnetic fraction (open squares) obtained from $(La_{0.67}Ca_{0.33})(Mn_{0.97}Sn_{0.03})O_{2.94}$ Mössbauer spectra. The meaning of dashed line is explained in the text. (b) Temperature variation of the $-\ln(f/f_0)$ parameter. The meaning of dashed line is explained in the text.

points show typical temperature dependences, resembling conventional magnetization curves. For a comparison, the temperature dependence of the experimental B_{hf}^{max} values was fitted with the theoretical function (dashed line in Fig. 2a) based on the molecular field theory applied to mixed-valent $Mn^{3.33+}$ with spin value

$S = 1.83$. Fitting this function to experimental points in Fig. 2a provided the value of the molecular field T_C^* equal to 160(3) K. This temperature is in good agreement with the T_C obtained from magnetization measurements defined as the extrapolation of the maximal slope of the magnetization curve to the temperature axis, which amounts to 158 K.

A decrease in the σ values of the $P(B_{hf})$ distributions (denoted by vertical lines around $\langle B_{hf} \rangle$ values in Fig. 2a) with increasing temperature is observed, in contrast to the $x = 0.01$ compound [6]. It is worth noting that the $\sigma/\langle B_{hf} \rangle$ ratio remains practically constant. One should also mention that the PM contribution appears at 145 K and reaches 100% for the 165 K spectrum, indicating an inhomogeneous character of the transition and the occurrence of the FM/PM phase segregation.

To shed some light on the dynamics of the Mn sublattice in this compound the $-\ln(f/f_0)$ parameter was calculated from the Mössbauer spectra (in the same way as in Ref. [6]), where f is the Lamb–Mössbauer factor and f_0 denotes f value at 15 K. It represents the mean square displacement difference ($\langle u^2 \rangle - \langle u_0^2 \rangle$, where $\langle u_0^2 \rangle$ corresponds to f_0 factor) of ^{119}Sn atoms. The temperature dependence of this parameter is presented in Fig. 2b. The theoretical dashed curve fitted to experimental points in this figure is based on a simple Debye model of the crystal [6] and gives the Debye characteristic temperature $\theta_D = 295(18)$ K.

3.2. NMR spectroscopy

^{55}Mn and ^{139}La NMR studies of the polycrystalline $(\text{La}_{0.67}\text{Ca}_{0.33})(\text{Mn}_{1-x}\text{Sn}_x)\text{O}_{2.94}$ ($x = 0$, 0.01, and 0.03) powder samples were performed using an automated frequency swept spectrometer [9]. Measurements were carried out at no applied magnetic field at the temperatures 4.2 K and 77 K. The spin-echo spectra were obtained by measuring the integrated echo intensity versus frequency. A pulse sequence consisting of two radio frequency pulses, $90°\text{-}\tau\text{-}180°$, was used. The pulse length t (0.1 μs $< t <$ 3 μs) and the pulse amplitude were adjusted to obtain a maximum echo signal at a given temperature. The resonant response of nuclear magnetic moments at Mn, La atomic sites in magnetic materials occurs at a frequency ν given by $\nu = \left(\frac{\gamma}{2\pi} \right) B_{hf}$, where γ is the nuclear gyromagnetic ratio and B_{hf} is the effective hyperfine magnetic field ($\gamma/2\pi = 10.501$ MHz/T for ^{55}Mn and 6.014 MHz/T for ^{139}La).

Figure 3 presents ^{55}Mn NMR spin-echo spectra at zero applied field for $(\text{La}_{0.67}\text{Ca}_{0.33})(\text{Mn}_{1-x}\text{Sn}_x)\text{O}_{2.94}$ compounds with $x = 0$, 0.01, and 0.03, measured at 4.2 K and 77 K. The $(\text{La}_{0.67}\text{Ca}_{0.33})\text{MnO}_{2.94}$ spectrum at 4.2 K shows a single broad resonant line positioned at 383.9(2) MHz (which corresponds to $B_{hf} = 36.56(2)$ T). The value of the resonant frequency was obtained from fitting single Gaussian function to the spectra. The observed single line spectrum in this metallic FM compound arises from a fast hopping of electrons (at a rate faster than the NMR Larmor frequency) due to the DE interaction between Mn^{3+} and Mn^{4+}. It results in a resonant frequency corresponding to an average $\text{Mn}^{3+/4+}$ state. The
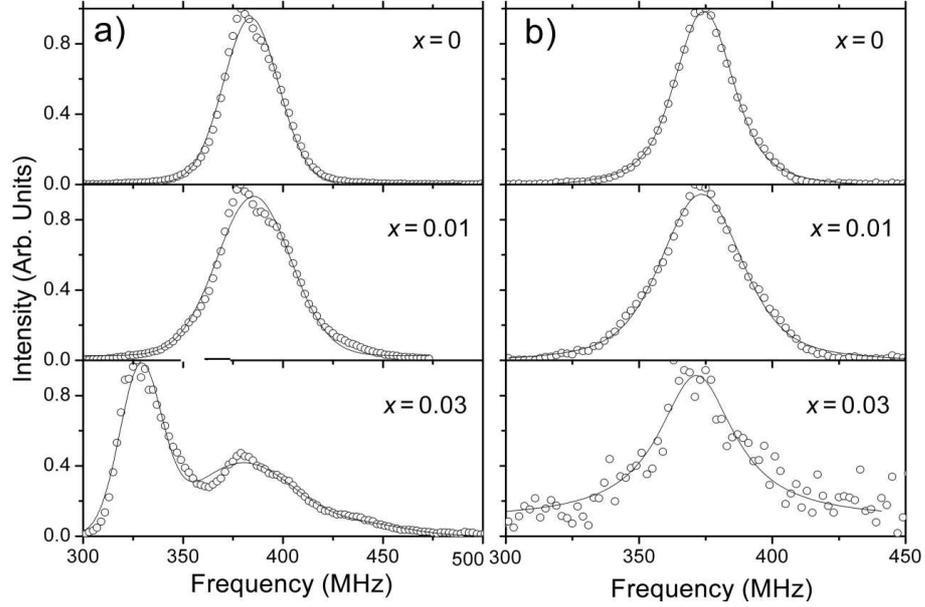
Fig. 3. Normalised ^{55}Mn NMR spin-echo spectra for $(La_{0.67}Ca_{0.33})(Mn_{1-x}Sn_x)O_{2.94}$ with $x = 0$, 0.01, and 0.03 at 4.2 K (a) and 77 K (b). Solid lines denote the single or multicomponent Gaussian fits to the spectra.

more complicated spectrum of $(La_{0.67}Ca_{0.33})(Mn_{0.97}Sn_{0.03})O_{2.94}$ at 4.2 K was fitted by three Gaussian lines according to the following interpretation. The central line with a similar shape and position (380(1) MHz) as in $(La_{0.67}Ca_{0.33})MnO_{2.94}$ was ascribed to an average $Mn^{3+/4+}$ state in the FM metallic regions of the sample. The sharpest and strongest line at 328.8(2) MHz (31.21(2) T) and the weakest and widest one at about 445(9) MHz (42.4(9) T) are attributed to the Mn^{4+} and Mn^{3+} charge localised states, respectively. One can justify this interpretation recalling that the ^{55}Mn nucleus in a magnetically ordered material experience a local field (neglecting dipolar fields contribution) given by

$$B_{hf} = g\mu_B\Big(A\langle S\rangle + \sum_j T_j\langle S_j\rangle\Big) + B_{ext}, \qquad (1)$$

where B_{ext} is the external field, $\langle S\rangle$, $\langle S_j\rangle$ are the on-site and nearest-neighbour electron spins and A, T_j are the hyperfine coupling constants. Ignoring the relatively small transferred contribution from the six Mn nearest neighbours ($\langle S_j\rangle$) to the local field (and at $B_{ext} = 0$), the approximate proportionality of the ^{55}Mn B_{hf} to the electronic spin $\langle S\rangle$ is found ($B_{hf} = g\mu_B A\langle S\rangle$). Since $\langle S\rangle$ for Mn^{3+} ion is 2 and for Mn^{4+} ion is 1.5, the ratio of the corresponding B_{hf} should be close to 1.33. The calculated 42.4 T/31.21 T ratio (1.36) supports this interpretation. The Mn^{3+}, Mn^{4+} resonant lines originate from the FM insulating phase in this compound. The $(La_{0.67}Ca_{0.33})(Mn_{0.99}Sn_{0.01})O_{2.94}$ spectrum at 4.2 K is

characterised by the wide line centred at 385.4(3) MHz (36.70(3) T). It has intermediate character with respect to the two above discussed spectra and shows a much smaller contribution of the FM insulating phase. At 77 K, only $Mn^{3+/4+}$ DE line was detected for $x = 0$, 0.01, and 0.03 compounds (see Fig. 3b) at frequencies 374.32(8) MHz, 373.4(2) MHz, and 371.5(7) MHz, respectively. A much smaller magnitude of the signal observed for $x = 0.03$ at 77 K than for other compounds indicates a very small content of the FM metallic phase in this compound.

The ^{139}La NMR spin-echo spectra for $x = 0$, 0.01, and 0.03 compounds at 4.2 K are shown in Fig. 4. As the on-site La electron spin $\langle S^{La} \rangle$ is equal to zero, according to Eq. (1), the La nucleus experiences only a transferred B_{hf} from the eight nearest-neighbour Mn $\langle S_j \rangle$ spins ($B_{hf} = g\mu_B \sum_j T_j \langle S_j \rangle$, at $B_{ext} = 0$) and gives information about transferred B_{hf} from Mn sublattice. One should note that similarly to ^{119}Sn Mössbauer spectroscopy, where on-site electronic spin $\langle S^{Sn} \rangle$ is also equal to zero, the B_{hf} is transferred from the six nearest-neighbour Mn $\langle S_j \rangle$ spins.
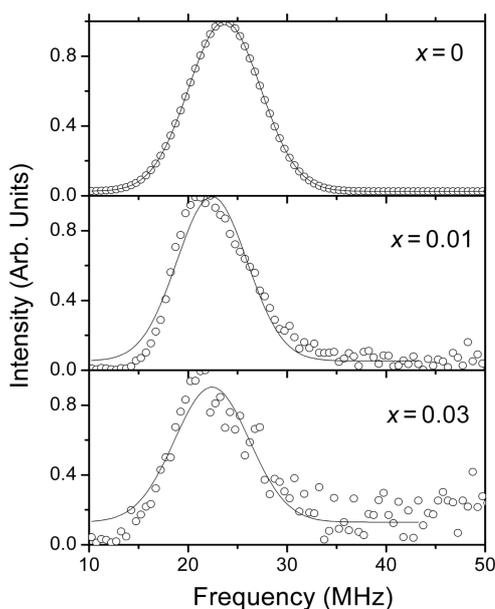
Fig. 4.   Normalised ^{139}La NMR spin-echo spectra for $(La_{0.67}Ca_{0.33})(Mn_{1-x}Sn_x)O_{2.94}$ with $x = 0$, 0.01, and 0.03 at 4.2 K. Solid lines denote the Gaussian fits to the spectra.

The spectra consist of a single broadened line centred at frequencies ranging from 23.69(5) MHz for $x = 0$ to 22.4(2) MHz for $x = 0.03$. A clearly asymmetrical shape is observed for $x = 0.01$ and $x = 0.03$ spectra.

The spin–spin relaxation time (T_2) for ^{55}Mn NMR spin-echo spectra was studied by measuring the echo amplitude at selected frequencies as a function of

the delay between the two pulses. Except for the $x = 0.03$ compound, these data measured at 4.2 K and 77 K could not be satisfactorily fitted by a single exponential relaxation function $(A_1 \exp(-2t/T_2))$ and usually two or three exponents with $10\ \mu s < T_2 < 160\ \mu s$ were necessary. This could be attributed to the coexistence of signals from domain walls and domains. In order to study T_2 relaxation more systematically, the ^{55}Mn spectra for $x = 0$, 0.01, and 0.03 compounds were measured for various pulse spacing τ. The set of such spectra measured at 4.2 K for $x = 0$ is shown in Fig. 5a. With increasing τ the appearance of a dip at the centre of the DE line and its gradual growing is observed. It reveals a minimum of T_2 at the centre of the resonant line due to the Suhl–Nakamura relaxation mechanism [10] resulting from indirect coupling of nuclear spins mediated by virtual spin waves. A similar variation of the spectra as a function of τ is found for $x = 0.01$ compound at 4.2 K. This is shown in the upper part of Fig. 5b. Similar but less pronounced Suhl–Nakamura relaxation effects are observed in the spectra measured at 77 K for $x = 0$ and $x = 0.01$ compounds. Such relaxation effects are not observed in the spectra of $x = 0.03$ compound at 4 K, shown in the lower part of Fig. 5b. A fast decrease in the intensity of the Mn^{3+} and Mn^{4+} lines in comparison with the DE $Mn^{3+/4+}$ line with increasing pulse-spacing indicates much shorter T_2 relaxation times for the FM insulating phase.
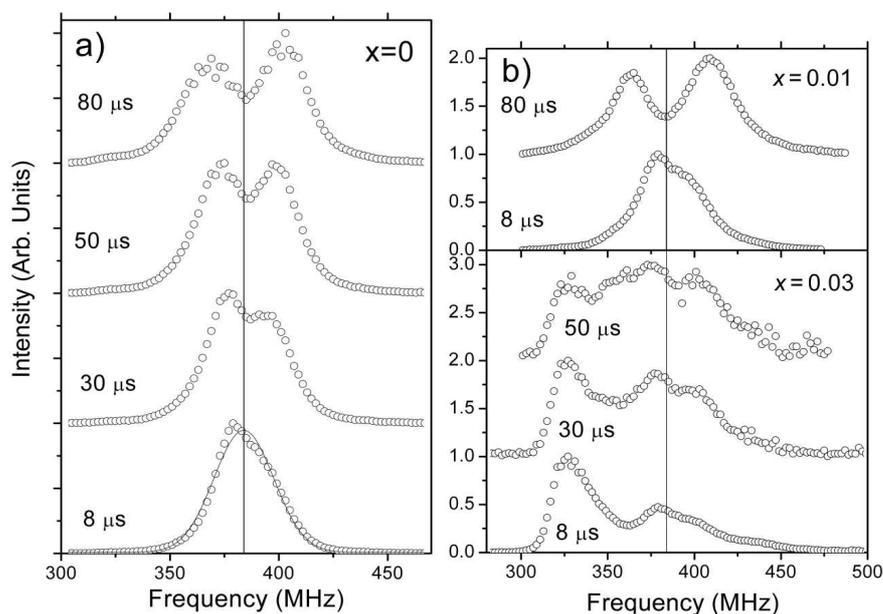
Fig. 5.   Pulse-spacing (τ) dependence of the normalised ^{55}Mn NMR spin-echo spectra for $(La_{0.67}Ca_{0.33})(Mn_{1-x}Sn_x)O_{2.94}$ with $x = 0$ (a), and $x = 0.01$, 0.03 (b), at 4.2 K. Solid line denotes the Gaussian fit to the $x = 0$ spectrum with $\tau = 8\ \mu s$.

Analysing properties of $(La_{0.67}Ca_{0.33})(Mn_{1-x}Sn_x)O_{3-\delta}$ at different levels x of doping Sn for Mn one should first consider the effects of oxygen deficiency δ on the parent compound. The positive value of δ (0.06) decreases the effective hole doping by amount of 2δ (0.12) and an equivalent doping with Ca would be obtained for oxygen stoichiometric compound $(La_{0.79}Ca_{0.21})MnO_3$. Such a compound locates very close to the border of stability of the FM metallic phase on the $(La,Ca)MnO_3$ phase diagram [4, 11]. Sn doping has a similar effect on the valency of the Mn atoms but in this case tetravalent Sn substitutes solely for Mn atoms. To keep charge neutrality of the compound, the relation $3.21 = 4x + (1 - x)V_{Mn}$ has to be fulfilled, where V_{Mn} is the valence state of Mn atoms. Making use of this relation, one can find for Sn substitution levels $x = 0.01$ and $x = 0.03$, V_{Mn} equal to 3.202 and 3.186, respectively. The first value corresponds to $(La_{0.798}Ca_{0.202})MnO_3$, and, looking on its physical properties, they correspond practically to the border line separating FM metallic state from the FM insulating state. The second V_{Mn} value corresponds to $(La_{0.814}Ca_{0.186})MnO_3$ which locates already below this border line, inside the FM insulating region. The proximity of the $(La_{0.67}Ca_{0.33})MnO_{2.94}$ compound to the FM metal–FM insulator border explains its large sensitivity to relatively low levels of Sn doping and allows us to understand most of the physical properties of $(La_{0.67}Ca_{0.33})(Mn_{1-x}Sn_x)O_{2.94}$ compounds. Positive, and similar for all the compounds studied, value of δ parameter is related to the existence of similar level of oxygen vacancies, which introduce local structural distortions and electronic inhomogeneities.

Substitution of Sn^{4+} for Mn^{4+} leads to a further increase in Mn^{3+}/Mn^{4+} ratio and to a suppression of the DE interactions and metallic conductivity, which manifests in decreasing both T_C and T_{M-I}. In addition, large Sn^{4+} ions introduce local structural distortions and microscopic strains which promote electronic phase segregation and cause an increase in the separation between these temperatures. This separation is substantial in $x = 0$ (18 K) and it increases in $x = 0.01$ to 66 K, where it achieves its maximum [3]. Such a behaviour is consistent with the $(La,Ca)MnO_3$ phase diagram proposed by Coey [11] in which the FM insulating phase appears in the narrow temperature range below T_C for x smaller than roughly 0.25 and with decreasing x the range of existence of this phase is considerably extending. The observed resistance changes near T_C in $x = 0$, 0.01 compounds were attributed to the "intrinsic" colossal magnetoresistance effect, which are opposed to the "extrinsic" effects observed at T_{M-I} and related to the scattering or tunnelling processes at the grain boundaries, inhomogeneities, and defects [3]. According to this interpretation the ground state for these compounds should be FM and metallic. This prediction was clearly confirmed by our ^{55}Mn NMR measurements on $x = 0$ and 0.01 compounds at 4.2 K and 77 K, where only single DE lines characteristic of FM metallic phase were detected. ^{55}Mn NMR measurements on $x = 0.03$ showed a completely different character of the ground state for this compound, in which the coexistence of the DE line, corresponding to

an average $Mn^{3+/4+}$ state with the lines characteristic of Mn^{3+} and Mn^{4+} valence states, takes place, similarly to those observed for $La_{0.9}Ca_{0.1}MnO_3$ compound [12]. This gives clear evidence for a local phase segregation in the compound at the timescale of the spin-echo NMR measurement, i.e. $t > 10^{-5}$ s.

4. Conclusions

The ^{119}Sn Mössbauer spectroscopy study revealed a different character of the FM state in the compound with $x = 0.03$ than with $x = 0$, 0.01. For $x = 0.01$ the ^{119}Sn B_{hf}^{max} remains finite at T_C determined from dc magnetization measurement and also the width of B_{hf} distribution is growing with increasing temperature [6].

For $x = 0$ and 0.01 the ^{55}Mn NMR [12] and ^{119}Sn Mössbauer measurements [6] provided the mean field T_C^* values much higher than the corresponding T_C obtained from dc magnetisation measurements. Similar results were also obtained for $(La_{0.67}Ca_{0.33})(Mn_{1-x}{}^{57}Fe_x)O_3$ with $x = 0$, 0.03, and 0.06 [13, 14]. For $x = 0.03$, on the contrary, the ^{119}Sn B_{hf}^{max} shows the fitted T_C^* value very close to T_C and the relative width of B_{hf} distribution remains constant with changing temperature.

Our ^{55}Mn NMR measurements on $x = 0$, 0.01, and 0.03 compounds confirm a different character of the FM ground state in $x = 0.03$ than in $x = 0$ or 0.01. The microscopically inhomogeneous FM state is most likely realized in the whole temperature range (for $T < T_C$) in $x = 0.03$. It is also possibly realized for $x = 0$ and 0.01 but in a much narrower temperature range between T_{M-I} and T_C [3, 11].

References

[1] C.N.R. Rao, A.K. Raychaudhuri, in: *Colossal Magnetoresistance, Charge Ordering and Related Properties of Manganese Oxides*, Eds. C.N.R. Rao, B. Raveau, World Scientific, Singapore 1998, p. 1.

[2] C. Zener, *Phys. Rev.* **82**, 403 (1951).

[3] J. Przewoźnik, J. Chmist, L. Kolwicz-Chodak, Z. Tarnawski, A. Kołodziejczyk, K. Krop, K. Kellner, G. Gritzner, *Acta Phys. Pol. A* **106**, 665 (2004).

[4] S.-W. Choeng, H.Y. Hwang, in: *Colossal Magnetoresistive Oxides*, Ed. Y. Tokura, Gordon and Breach, London 2000, p. 237.

[5] A. Simopoulos, G. Kallias, E. Devlin, I. Panagiotopoulos, M. Pissas, *J. Magn. Magn. Mater.* **177-181**, 860 (1998).

[6] J. Przewoźnik, J. Żukrowski, J. Chmist, E. Japa, A. Kołodziejczyk, K. Krop, K. Kellner, G. Gritzner, *Nukleonika* **49**, S37 (2004).

[7] J. Hesse, A. Rübartch, *J. Phys. E, Sci. Instrum.* **7**, 526 (1974).

[8] G. Le Caer, J.M. Dubois, *J. Phys. E, Sci. Instrum.* **12**, 1083 (1979).

[9] S. Lord, P.C. Riedi, *Meas. Sci. Technol.* **6**, 149 (1999).

[10] M.M. Savosta, P. Novak, *Phys. Rev. Lett.* **87**, 137204 (2001).

[11] J.M.D. Coey, *Adv. Phys.* **48**, 167 (1999).

[12] Cz. Kapusta, P.C. Riedi, W. Kocemba, M.R. Ibarra, J.M.D. Coey, *J. Appl. Phys.* **87**, 7121 (2000).

[13] J. Przewoźnik, Cz. Kapusta, J. Żukrowski, K. Krop, M. Sikora, D. Rybicki, D. Zając, C.J. Oates, P.C. Riedi, *Phys. Status Solidi B* **243**, 259 (2006).

[14] J. Przewoźnik, J. Żukrowski, J. Chmist, Z. Tarnawski, A. Kołodziejczyk, K. Krop, K. Kellner, G. Gritzner, *Phys. Status Solidi C* **3**, 138 (2006).